

The magneto-optical Franz-Keldysh effect of a two-dimensional electron gas in high magnetic fields and intense terahertz laser fields in Faraday geometry

This article has been downloaded from IOPscience. Please scroll down to see the full text article.

2001 J. Phys.: Condens. Matter 13 10889

(<http://iopscience.iop.org/0953-8984/13/48/314>)

View [the table of contents for this issue](#), or go to the [journal homepage](#) for more

Download details:

IP Address: 171.66.16.238

The article was downloaded on 17/05/2010 at 04:37

Please note that [terms and conditions apply](#).

The magneto-optical Franz–Keldysh effect of a two-dimensional electron gas in high magnetic fields and intense terahertz laser fields in Faraday geometry

W Xu^{1,2} and L B Lin²

¹ Department of Engineering Physics, University of Wollongong, Wollongong NSW 2522, Australia

² Department of Physics, Sichuan University, Chengdu-610064, People's Republic of China

E-mail: wxu@wampus.its.uow.edu.au

Received 22 May 2001, in final form 8 October 2001

Published 16 November 2001

Online at stacks.iop.org/JPhysCM/13/10889

Abstract

We present a theoretical study on the density of states (DoS) of a two-dimensional electron gas subjected simultaneously to an intense laser field and a strong perpendicular magnetic field. We find that in the Faraday geometry, due to the coupling of the magnetic field to the laser field, the DoS of a Landau level (LL) is split into a series of peaks centred at $E = E_N + (eF_0)^2/[4m^*(\omega^2 - \omega_c^2)] + m\hbar\omega$. Here, ω and F_0 are respectively the frequency and the electric field strength of the laser field, ω_c is the cyclotron frequency, E_N is the N th LL energy, and $m = 0, \pm 1, \pm 2, \dots$ corresponding to different optical processes. This is electrically analogous to the Franz–Keldysh effect for an electron gas driven by a strong external field and we therefore name it the magneto-optical Franz–Keldysh effect.

1. Introduction

It is well known that when a two-dimensional electron gas (2DEG) is subjected to strong perpendicular magnetic fields in the absence of intense electromagnetic (EM) radiation, due to Landau quantization, the density of states (DoS) of the 2DEG is a series of peaks centred at each Landau level (LL) with energy $E = E_N = (N + 1/2)\hbar\omega_c$, where $N = 0, 1, 2, \dots$, $\omega_c = eB/m^*$ is the cyclotron frequency, and m^* is the effective electron mass. This results in important observations [1] such as Shubnikov–de Haas oscillations and quantum Hall effects. With the development and application of state-of-the-art intense laser technologies such as that of free-electron lasers (FELs), it has now become possible to investigate the interactions between electrons and intense laser fields in 2DEG systems in the presence of quantizing magnetic fields. This has opened up a new field of research in magneto-optics and magneto-transport. The FELs are generated by passing an intense beam of relativistic electrons through

periodic magnetic fields and the current generation of the FELs can provide a high-power, frequency-tunable, and linearly polarized laser radiation source of terahertz³ (10^{12} Hz or THz) bandwidth [2]⁴. Recently, experimental work has been conducted to study magneto-optical and magneto-transport properties in GaAs-based 2DEGs in quantizing magnetic fields and THz FEL fields [3, 4]. Unusual and important THz radiation phenomena, such as the photon-enhanced high-temperature cyclotron resonance (CR) effect [3], photon-modified Shubnikov–de Haas oscillation, and quantum Hall effects [4], have been observed using magneto-transport measurements. These new experimental findings suggest strongly that the field of electron interactions with intense THz laser radiation in high magnetic fields is very rich in terms of physics and in device applications.

Like in other studies, in the investigation of magneto-optical and magneto-transport properties of a 2DEG in strong magnetic fields and intense laser fields, the electron DoS is one of the central quantities required to determine and to understand almost all physically measurable properties. In the Voigt geometry where the laser field does not couple directly to the magnetic field, the DoS of a 3DEG was studied theoretically by Xu, and important radiation effects, such as the dynamical Franz–Keldysh effect (DFKE), were observed [5]. At present, little is known theoretically about how an intense laser radiation affects the DoS of the LLs in a 2DEG in the Faraday geometry where the laser field couples directly to the magnetic field. In view of the fact that currently most experimental measurements on 2DEGs in FEL fields and high magnetic fields are carried out in the Faraday geometry [3, 4], it is of value to examine the influence of the intense laser radiation on the DoS of the 2DEG in this unique configuration. In this paper, we present a detailed theoretical study of how electrons in a 2DEG respond to linearly polarized intense THz laser fields in the presence of strong static magnetic fields in the Faraday geometry. In section 2, on the basis of a time-dependent condensed matter theory, we consider a simple theoretical treatment to calculate the steady-state DoS of a 2DEG in coupled magnetic and EM fields. The main theoretical results are presented and discussed in section 3, and the conclusions drawn from this study are summarized in section 4.

2. Theoretical approaches

2.1. Solution of the Schrödinger equation

In this paper, we employ a non-perturbative approach to obtain the DoS of a 2DEG in the presence of strong magnetic fields and intense laser fields in the Faraday geometry. We consider the situation where: (i) a 2DEG is formed along the xy -plane and the growth direction of the 2DEG is along the z -axis; (ii) a magnetic field B is applied perpendicular to the 2D plane of the 2DEG (e.g., applied along the z -axis); and (iii) a laser field $A_x(t)$ is applied along the z -axis and is polarized linearly along the x -direction. In this configuration (known as the Faraday geometry), the magnetic and laser fields do not couple to the confinement potential of the 2DEG and the magnetic field couples directly to the linearly polarized laser field. As a result, the CR effect can be immediately expected. In this case, there is no gauge in which the electron Hamiltonian is translationally invariant [6] and the most convenient gauge for describing the two uniform fields is

$$\phi(\mathbf{R}, t) = 0 \quad \text{and} \quad \mathbf{A}(\mathbf{R}, t) = (A_x(t), -Bx, 0) \quad (1)$$

where $\mathbf{R} = (\mathbf{r}, z) = (x, y, z)$. Here, we have used the Landau gauge and the Coulomb gauge for the vector and scalar potentials induced respectively by the static magnetic field and by the

³ $f = 1$ THz in frequency is $299.79 \mu\text{m}$ in wavelength, 4.14 meV in energy, and 47.99 K in temperature. For GaAs, 1 THz is 2.38 T in magnetic field.

⁴ For the recent development of the FELs, see, e.g., [2].

EM radiation field. It should be noted that the usage of the Coulomb gauge for the radiation field can also satisfy the conditions for free electrons, such as the charge density and the current density being zero when scattering, inhomogeneities, external driving fields, etc, are absent [7].

After using the dipole approximation for the EM field, we can write $A_x(t) = A_0 \sin(\omega t)$, where ω is the frequency of the radiation and $A_0 = F_0/\omega$, with F_0 being the electric field strength of the EM field. Thus, the electron Hamiltonian for a 2DEG can be written as

$$H(t) = H_{xy}(t) + H_z \quad (2.1)$$

where

$$H_{xy}(t) = \frac{1}{2m^*} [(p_x - eA_x(t))^2 + (p_y + eBx)^2] \quad (2.2)$$

and

$$H_z = \frac{p_z^2}{2m^*} + U(z). \quad (2.3)$$

Here, m^* is the effective electron mass, $p_x = -i\hbar \partial/\partial x$ is the momentum operator along the x -direction, and $U(z)$ is the confinement potential energy of the 2DEG along the growth direction. The time-dependent Schrödinger equation

$$i\hbar \partial\Psi(\mathbf{R}, t)/\partial t = H(t)\Psi(\mathbf{R}, t) \quad (3)$$

can be solved analytically and the time-dependent electron wavefunction is obtained as (see appendixes A and B)

$$\Psi_{N,k_y,n}(\mathbf{R}, t) = \Phi_{N,k_y,n}(\mathbf{r}, t)\psi_n(z) \quad (4.1)$$

where

$$\Phi_{N,k_y,n}(\mathbf{r}, t) = e^{ik_y y} e^{-iE_{em}\tau_0(t)/\hbar} e^{-i(E_N + \varepsilon_n + E_{em})t/\hbar} \chi_N(x - X) e^{ix_0(x-X)/l^2}. \quad (4.2)$$

Here, k_y is the electron wavevector along the y -direction, $X = X(t) = -l^2 k_y + x_1(t)$ with $l = (\hbar/eB)^{1/2}$ being the radius of the ground cyclotron orbit, and $E_N = (N + 1/2)\hbar\omega_c$ is the N th LL energy with $N = 0, 1, 2, \dots$ and $\omega_c = eB/m^*$ being the cyclotron frequency. In equation (4.2)

$$\begin{aligned} x_0 &= x_0(t) = -\frac{eF_0}{m^*\omega} \frac{\omega_c \sin(\omega t) - \omega \sin(\omega_c t)}{\omega^2 - \omega_c^2} \\ x_1 &= x_1(t) = \frac{eF_0}{m^*} \frac{\cos(\omega t) - \cos(\omega_c t)}{\omega^2 - \omega_c^2} \\ \tau_0(t) &= \frac{\omega_c^2/\omega}{\omega^2 - \omega_c^2} \left[\frac{3\omega_c^2 - \omega^2}{2\omega_c^2} \sin(2\omega t) + \frac{\omega}{\omega_c} \sin(2\omega_c t) - 4 \sin(\omega t) \cos(\omega_c t) \right]. \end{aligned}$$

Also,

$$E_{em} = \frac{(eF_0)^2}{4m^*(\omega^2 - \omega_c^2)}$$

is an energy induced by the radiation and magnetic fields, and

$$\chi_N(x) = (2^N N! \pi^{1/2} l)^{-1/2} e^{-(x/l)^2/2} H_N(x/l)$$

with $H_N(x)$ being the Hermite polynomials. Furthermore, because the applied magnetic and laser fields do not couple with the confining potential of the 2DEG, the electron wavefunction along the growth direction, $\psi_n(z)$, and the energy of the n th electronic subband, ε_n , are determined by the time-independent Schrödinger equation along the z -direction: $[H_z - \varepsilon_n]\psi_n(z) = 0$.

2.2. The Green function for electrons

With the time-dependent electron wavefunction, we can derive the retarded propagator or Green function for electrons in different representations. In this paper, we generalize a common approach used in time-dependent condensed matter theory [8] to derive the Green function. Because the Hamiltonian $H_{xy}(t)$ can only be solved in real space, we can first write the electron Green function for the n th subband in the (\mathbf{r}, t) or (space, time) representation as

$$G_n(\mathbf{r}, t; \mathbf{r}', t') = -\frac{i}{\hbar} \Theta(t - t') \sum_{N, k_y} \Phi_{N, k_y, n}^*(\mathbf{r}', t') \Phi_{N, k_y, n}(\mathbf{r}, t) \quad (5)$$

which satisfies

$$\left[i\hbar \frac{\partial}{\partial t} - H_{xy}(t) + \varepsilon_n \right] G_n(\mathbf{r}, t; \mathbf{r}', t') = \delta(t - t') \delta(\mathbf{r} - \mathbf{r}'). \quad (6)$$

After summing over k_y , we have

$$\begin{aligned} G_n(\mathbf{r}, t; \mathbf{r}', t') &= -\frac{i}{\hbar} \frac{\Theta(t - t')}{2\pi l^2} \sum_N e^{-Y/2} L_N(Y) e^{-i(E_N + \varepsilon_n + E_{em})(t - t')} \\ &\times e^{-iE_{em}[\tau_0(t) - \tau_0(t')]/\hbar} e^{i[x_0(t) + x_0(t')][x - x' - x_1(t) + x_1(t')]/2l^2} \\ &\times e^{-i[x + x' - x_1(t) - x_1(t')](y - y')/2l^2} \end{aligned} \quad (7)$$

with $Y = [(x - x' - x_1(t) + x_1(t'))^2 + (y - y' + x_0(t) - x_0(t'))^2]/2l^2$ and $L_N(x) = L_N^0(x)$ being the Laguerre polynomials.

From equation (7), we see that due to the coupling between the magnetic field and the EM field, the Green function depends not only on $r - r'$ but also on $r + r'$. Thus, the Green function in (\mathbf{k}, t) or (momentum, time) representation should be derived from space Fourier transform of $G_n(\mathbf{r}, t; \mathbf{r}', t')$ in relation to relative coordinates $r - r'$ and to space centre-of-mass coordinates $(r + r')/2$. On doing this, the Green function for the n th subband in the (\mathbf{k}, t) representation is obtained as

$$\begin{aligned} G_n(\mathbf{k}; t, t') &= -\frac{i}{\hbar} \Theta(t - t') 2e^{-i[x_0(t) + x_0(t')][x_1(t) - x_1(t')]/2l^2} e^{i[(x_1(t) - x_1(t'))k_x^* - (x_0(t) - x_0(t'))k_y^*]} \\ &\times e^{-iE_{em}[\tau_0(t) - \tau_0(t')]/\hbar} \sum_N (-1)^N e^{-i(E_N + \varepsilon_n + E_{em})(t - t')/\hbar} \\ &\times e^{-l^2(k_x^{*2} + k_y^{*2})} L_N[2l^2(k_x^{*2} + k_y^{*2})] \end{aligned} \quad (8)$$

where $k_x^* = k_x + [x_0(t) + x_0(t')]/2l^2$ and $k_y^* = k_y + [x_1(t) + x_1(t')]/2l^2$.

After averaging $G_n(\mathbf{k}; t, t')$ over \mathbf{k} , we obtain the Green function for the n th subband in the time representation:

$$G_n(t, t') = G_n(\tau, T) = -\frac{i}{\hbar} \frac{\Theta(\tau)}{2\pi l^2} \sum_N e^{-i(E_N + \varepsilon_n + E_{em})\tau/\hbar} e^{-iA} e^{-B/2} L_N(B) \quad (9)$$

where $\tau = t - t'$ is the time 'relative coordinates', $T = (t + t')/2$ is the time 'centre-of-mass coordinates',

$$A = \frac{E_{em}}{\hbar\omega} \left[\frac{2\omega_c^2}{\omega^2 - \omega_c^2} - \cos(2\omega T) \right]$$

and

$$B = \frac{4E_{em}\omega_c}{\hbar\omega^2} \left[\frac{\omega^2 + \omega_c^2}{\omega^2 - \omega_c^2} - \cos(2\omega T) \right] \sin^2\left(\frac{\omega\tau}{2}\right).$$

From a theoretical perspective, when a time-dependent potential such as an EM potential is present, the electronic quantities in general are two-time ones. In this case, the response of an electron to the time-dependent driving field depends not only on the time difference $t - t'$ but also on the time shift (e.g., $t + t'$) induced by the applied external field. This feature has been reflected in the electron Green function in the time representation.

To investigate the steady-state property of a two-time quantity $F(t, t')$ in the presence of a time-dependent periodic field, the most convenient and popularly used theoretical approach [9] is first Fourier analysing $F(t, t') = F(\tau, T)$ along the τ -direction to get $F(\Omega, T)$, then averaging T in $F(\Omega, T)$ over a period of the driving field to get $F(\Omega)$ in the spectrum representation. The Fourier transform (or average over time τ) of $G_n(\tau, T)$ is given by

$$G_n(E, T) = \frac{1}{2\pi l^2} \sum_N \sum_{m=-\infty}^{\infty} \frac{F_{Nm}(\cos(2\omega T))}{E - E_N - \varepsilon_n - E_{em} - m\hbar\omega + i\delta} \quad (10)$$

where an infinitesimal quantity $i\delta$ has been introduced to make the integral converge, E is the electron energy, and (see appendix C)

$$F_{Nm}(y) = \frac{(-1)^m}{\pi} \int_0^\pi dx \cos(mx + C \sin x) e^{-\mathcal{D}(1+\cos x)/4} L_N \left(\frac{\mathcal{D}}{2} (1 + \cos x) \right)$$

with

$$C = \frac{E_{em}}{\hbar\omega} \left[\frac{2\omega_c^2}{\omega^2 - \omega_c^2} - y \right] \quad \text{and} \quad \mathcal{D} = \frac{4E_{em}\omega_c}{\hbar\omega^2} \left[\frac{\omega^2 + \omega_c^2}{\omega^2 - \omega_c^2} - y \right].$$

In equation (10), m is induced by the Fourier transform and corresponds to emission and absorption of photons with energy $m\hbar\omega$. Therefore, m is an index for different optical channels, i.e., $m > 0$ ($m < 0$) for m -photon absorption (emission) and $m = 0$ for elastic optical process. By averaging T in equation (10) over a period of the radiation field, the Green function for the n th subband in spectrum representation is obtained as

$$G_n(E) = \frac{1}{2\pi l^2} \sum_N \sum_{m=-\infty}^{\infty} \frac{F_{Nm}}{E - E_N - \varepsilon_n - E_{em} - m\hbar\omega + i\delta} \quad (11)$$

where $F_{Nm} = (1/2\pi) \int_0^{2\pi} dx F_{Nm}(\cos(2x))$ and the degeneracy of each LL is given by $1/2\pi l^2$.

2.3. Density of states

The steady-state electron DoS is defined from the imaginary part of the retarded Green function in the spectrum representation. The total DoS of a 2DEG is given by

$$D(E) = -\frac{g_s}{\pi} \sum_n \text{Im} G_n(E) = \frac{g_s}{2\pi l^2} \sum_{N,n} \sum_{m=-\infty}^{\infty} F_{Nm} \delta(E - E_N - \varepsilon_n - E_{em} - m\hbar\omega) \quad (12)$$

where $g_s = 2$ accounts for the spin degeneracy.

3. Results and discussion

3.1. Analytical results

From equation (12), we see that, similarly to the case where the radiation field is not applied, the presence of a quantizing magnetic field leads to a singular nature of the DoS of a 2DEG in the absence of scattering. This singular nature is characterized by a series of δ -function peaks centred at $E = E_N + \varepsilon_n + E_{em} + m\hbar\omega$. In the presence of scattering, inhomogeneities, etc, the LLs are broadened and the singularities of the DoS are damped. To our knowledge, at present little is known about the shift and broadening of the LLs induced by electronic scattering

mechanisms in the presence of intense radiation fields. In this paper, we limit ourselves to the case of the electron DoS caused by direct coupling between magnetic field and laser radiation and we neglect the details of the LL structure induced by electronic scattering channels. It has been demonstrated that in the absence of the radiation field, the DoS of the LLs for a 2DEG is basically semielliptic [10]. For a semielliptic type of DoS, equation (12) becomes

$$D(E) = \frac{2}{\pi^2 l^2} \sum_{N,n} \frac{1}{\Gamma_{Nn}} \sum_{m=-\infty}^{\infty} F_{Nm} \operatorname{Re} \left[1 - \left(\frac{E - E_N - \varepsilon_n - E_{em} - m\hbar\omega}{\Gamma_{Nn}} \right)^2 \right]^{1/2} \quad (13)$$

with Γ_{Nn} being the width of the N th LL in the n th subband.

In the non-perturbative approach developed in this paper to obtain the Green function for electrons and the electron DoS, the effects of the magnetic and radiation fields are included exactly. In an electronic system, when the magnetic field couples to the radiation field, the CR effect should be present. This can be seen in the time-dependent electron wavefunction (equation (4)), the Green function for the electrons (equations (7)–(11)), and in the electron DoS (equations (12) and (13)). In the presence of an intense radiation field, electrons in the system can interact with the radiation field via absorption and emission of photons, including multi-photon processes. This has been reflected in the Green function (equation (11)) and in the electron DoS (equation (13)), where a factor F_{Nm} plays a role in switching different optical channels for different LLs.

It is well known that when an electron gas is subjected to a strong dc field, the electron DoS will be blue-shifted by the energy of the electric field. As a consequence, the fundamental absorption edge will also be blue-shifted. This is known as the Franz–Keldysh effect (FKE) [11]. A similar phenomena occurs when an intense laser field is applied to an electron gas system, where the electron DoS and the fundamental absorption edge are blue-shifted [12, 13]⁵ by an energy $E_{em}|_{B=0} = (eF_0)^2 / (4m^* \omega^2)$ in the absence of a magnetic field. This is electrically analogous to the FKE and the effect has been named the DFKE [9]. Very recently, the blue-shift of the fundamental absorption edge by $E_{em}|_{B=0}$ in GaAs-based 2DEG systems has been successfully observed experimentally using THz FELs as intense laser radiation sources [14]. In the presence of a magnetic field and a linearly polarized laser field in the Faraday geometry, the coupling of the magnetic and radiation fields to the 2DEG system results in the energy of the system being shifted by the energy $E_{em} + m\hbar\omega$. This implies that for a 2DEG subjected to a strong magnetic field and an intense laser field, the electron DoS will be split into a series of peaks according to different optical processes and will be shifted by the energy $E_{em} + m\hbar\omega$. As a result, we expect the fundamental absorption edge to also be shifted by $E_{em} + m\hbar\omega$. Thus, for the present situation, the FKE should be observed through the shift of the fundamental absorption edge by an energy $(eF_0)^2 / [4m^*(\omega^2 - \omega_c^2)] + m\hbar\omega$. Since this effect occurs in the presence of coupled magnetic and laser fields and is fundamentally different from those observed in the absence of the magnetic field, we name it here the magneto-optical Franz–Keldysh effect (MOFKE).

In contrast to the DFKE observed in the absence of a magnetic field, where only a blue-shift can be observed for elastic optical processes (i.e., for $m = 0$ where the maximum electron DoS can be observed), the presence of the magnetic field will lead to the phenomenon that both blue-shifts ($\omega > \omega_c$) and red-shifts ($\omega < \omega_c$) can be measured for $m = 0$ in the MOFKE. When the condition of the CR is satisfied, i.e., $\omega \sim \omega_c$, the electronic transitions are mainly achieved via inter-LL transition events and the shift of the MOFKE cannot be measured. The CR effect can be seen from the energy shift E_{em} induced by the radiation and magnetic fields and from the factor F_{Nm} for different LLs and different optical processes.

⁵ For case of a 3DEG, see [12]; for case of a 2DEG, see [13].

Moreover, as demonstrated in, e.g., [9], the time-dependent Green function obtained for an electron gas in intense laser fields can be used to derive, e.g., the dielectric response function. The Green function given by equation (5) can also be applied to derive the electron density–density correlation function and the RPA dielectric function for a 2DEG subjected to high magnetic fields and intense laser fields⁶. In this paper, we limit ourselves to the discussion of the electron DoS resulting from equation (5).

3.2. Numerical results

In this paper, the numerical calculations are carried out for GaAs-based 2DEG systems. The effective electron mass for GaAs is $m^* = 0.0665m_e$ with m_e being the rest electron mass. We consider a situation where one electronic subband is present in a 2DEG and we use results obtained from the self-consistent Born approximation for the LL width. Under the short-range scattering approximation, we have [15]

$$\Gamma_{Nn} = \Gamma = \left(\frac{2e\hbar^2\omega_c}{\pi\mu_0m^*} \right)^{1/2} \quad (14)$$

with μ_0 being the low-temperature electron mobility at $B = 0$. In the calculations, we take a typical value of $\mu_0 = 10 \text{ m}^2 \text{ V}^{-1} \text{ s}^{-1}$ to estimate the LL width and take a typical value of the electron density $n_e = 8 \times 10^{14} \text{ m}^{-2}$ to calculate the Fermi energy. Moreover, the optical channels for $m = 0, \pm 1, \pm 2, \dots, \pm 30$ are included in the calculations.

The electron DoS for the lowest LL, $N = 0$, $D_0(E)$, at a fixed magnetic field $B = 5 \text{ T}$ and a fixed radiation intensity⁷ $F_0 = 5 \text{ kV cm}^{-1}$ are shown in figures 1 and 2 for different radiation frequencies: $\omega < \omega_c$ in figure 1 and $\omega > \omega_c$ in figure 2. $F_0 = 0$ (dotted curves in figures 1 and 2) corresponds to the case where the radiation field is absent. From figures 1 and 2, we see that in the presence of a linearly polarized intense laser field and a quantizing magnetic field in the Faraday geometry:

- (i) the DoS of a LL for a 2DEG is split into a series of peaks centred at $E = E_N + E_{em} + m\hbar\omega$;
- (ii) the shift of the DoS from that at $F_0 = 0$ depends not only on the energy induced by coupled radiation and magnetic fields (E_{em}) but also on the event: absorption or emission of photons ($m\hbar\omega$);
- (iii) when a channel for elastic optical scattering (i.e., $m = 0$) opens up, the red-shifts and blue-shifts of the DoS caused by this optical process can be observed respectively at $\omega < \omega_c$ (figure 1) and at $\omega > \omega_c$ (figure 2);
- (iv) the electron DoS can be present in the lower- and even the negative-energy regime, due to the energy shift induced by E_{em} and to the presence of channels for optical emission; and
- (v) absorption ($m > 0$) and elastic ($m = 0$) optical scattering processes give the major contributions to the electron DoS, whereas a relatively weak effect can be observed for those caused by photon emission events.

These results indicate that when an intense laser field is applied to a 2DEG, the electron DoS differs significantly from that at $F_0 = 0$.

Experimentally, at low temperatures and in the absence of the laser radiation, the DoS of the 2DEGs has been successfully determined by measuring, e.g., equilibrium quantities such as magnetization [16], capacitance [17], specific heat [16], and magnetic susceptibility [18].

⁶ The results will be presented elsewhere.

⁷ The connection between the electric field strength of a laser field (F_0) and the laser output power (I) is: $I = 0.5\sqrt{\epsilon/\mu}|F_0|^2 \simeq 1.32|F_0|^2 \text{ kW cm}^{-2}$ where F_0 is in units of kV cm^{-1} .

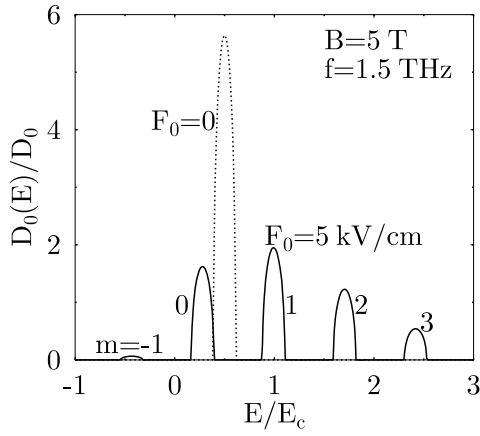


Figure 1. The electron DoS for the lowest LL $N = 0$ at a fixed magnetic field and a fixed radiation field where $\omega < \omega_c$. The electron energy is measured from $E = E + \varepsilon_0$, $m > 0$ ($m < 0$) corresponds to a channel for m -photon absorption (emission), $E_c = \hbar\omega_c$, and $D_0 = m^*/\pi\hbar^2$. $F_0 = 0$ (dotted curve) is the DoS in the absence of a radiation field.

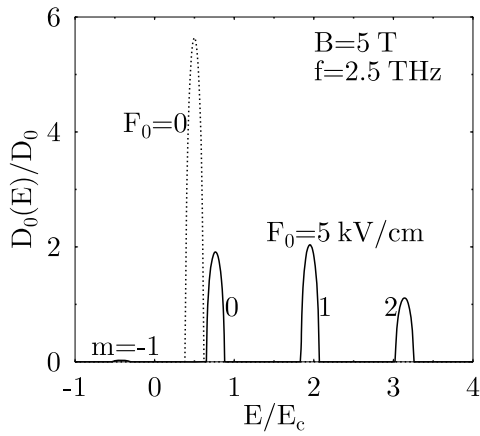


Figure 2. The electron DoS for the 0th LL at a fixed magnetic field and a fixed radiation field where $\omega > \omega_c$. The other parameters are the same as for figure 1.

Some of these experiments can also be used to determine the DoS of the 2DEG in the presence of quantizing magnetic fields and intense laser fields in the Faraday geometry. From the theoretical results shown above, we see that for GaAs-based 2DEG systems at a magnetic field of about $B \sim 1$ T, the strong modification and perturbation to the electron DoS by the radiation field can be observed when the radiation intensity $F_0 \sim 10 \text{ kV cm}^{-1}$ (or output power $P \sim 100 \text{ kW cm}^{-2}$) and radiation frequency $f \sim 1$ THz.

An important and direct application of the electron DoS is in determining the Fermi energy of an electronic system. We can estimate the Fermi energy E_F by assuming that the total electron density n_e in a 2DEG system is not varied by the presence of the radiation and magnetic fields, and by introducing the electron DoS into the condition of electron number conservation:

$$n_e = \int_{-\infty}^{\infty} f(E)D(E) dE \quad (15)$$

where $f(E)$ is the Fermi–Dirac function. The zero-temperature Fermi energy, measured from the energy E_{em} , is plotted in figure 3 as a function of magnetic field at a fixed radiation frequency for different radiation intensities. It should be noted that in the Faraday geometry, the CR effect can be seen in the Fermi energy. With increasing radiation intensity, a stronger CR effect is observed in the Fermi level. When $\omega_c > \omega$ ($\omega_c < \omega$) the Fermi energy increases (decreases) with increasing F_0 . Since E_{em} diverges when $\omega_c \sim \omega$, the results shown in figure 3

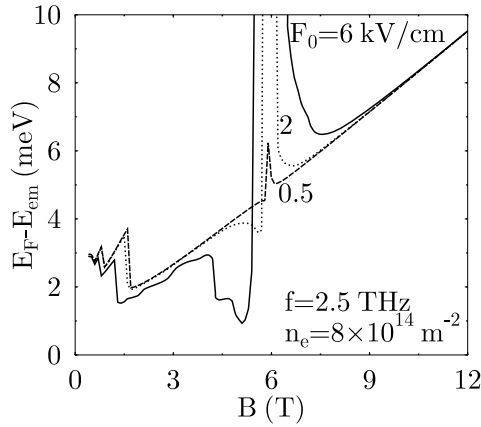


Figure 3. Zero-temperature Fermi energy, measured from the energy E_{em} , versus magnetic field at a fixed radiation frequency for different radiation intensities. n_e is the electron density of the 2DEG. Note that the CR effect occurs at $\omega_c \simeq \omega$.

imply that when the condition for the CR is satisfied, the Fermi energy of the system becomes infinity from a theoretical point of view. We note that in the model, we only consider an ideal situation with features such as a ‘pure’ radiation frequency and a ‘strict’ linear polarization of the radiation field. For real radiation sources, e.g., FELs, the radiation frequency can be slightly broadened and the linear polarization of the radiation can be slightly bent. These effects can damp the singular natures of the Fermi energy and other electronic properties when $\omega_c \sim \omega$.

4. Conclusions

When we consider a semiconductor-based 2DEG subjected simultaneously to quantizing magnetic fields and to intense THz laser fields, we enter a regime with different competing energies, such as the Fermi, cyclotron, and photon energies. These energies (frequencies) are of the order of meV (THz). This implies that the intense THz radiation can couple strongly to the electronic systems and, as a consequence, we can observe and study THz-photon-induced novel magneto-optical effects. In this paper, we have examined a rather simple and important phenomenon which may be observable using the state-of-the-art laser and high-magnetic-field technologies.

We have demonstrated that when a 2DEG is subjected to intense laser fields and to strong magnetic fields in the Faraday geometry, the DoS of a LL and, as a result, the fundamental absorption edge are split and shifted by an energy $E_{em} = (eF_0)^2/[4m^*(\omega^2 - \omega_c^2)]$ induced by the radiation and magnetic fields and by the energy transfer $m\hbar\omega$ due to different optical processes. In contrast to the DFKE observed for a 2DEG at $B = 0$, where only a blue-shift can be seen, we predict that in the presence of the strong magnetic fields, both red-shifts and blue-shifts of the MOFKE can be measured. For a semiconductor-based 2DEG system, the MOFKE can be observed when $B \sim 1$ T, $F_0 \sim 10$ kV cm $^{-1}$, and $\omega \sim 1$ THz. The radiation condition has been realized by the current generation of the THz FELs. Because the DFKE has been observed experimentally for GaAs-based 2DEGs [14], we hope that the phenomena discussed and predicted in this paper will also be verified experimentally.

Acknowledgments

One of us (WX) is a Research Fellow of the Australian Research Council (ARC). This work was also supported by the ARC IREX Grant, Visiting Scholar Foundation of Key Laboratory in the University of the Ministry of Education, China and National Natural Science Foundation of China.

Appendix A

It can be proven that when a static magnetic field is applied along the z -direction and is included within the Landau gauge, at an arbitrary gauge for describing a radiation field which is polarized linearly along the x -direction, the time-dependent Schrödinger equation can be transformed into a wave equation:

$$i\hbar \frac{\partial \Phi(x, t)}{\partial t} = \left[-\frac{\hbar^2}{2m^*} \frac{\partial^2}{\partial x^2} + \frac{m^*}{2} \omega_c^2 [x + f(t)]^2 \right] \Phi(x, t) \quad (\text{A.1})$$

where $f(t)$ can be a time-dependent arbitrary function. Using the canonical transformation proposed by Husimi [19], the solution of equation (A.1) is given by

$$\Phi(x, t) = \chi_N(x - x_0) \exp \left[-\frac{i}{\hbar} \left(E_N t - m^* \left[(x - x_0) \frac{dx_0}{dt} + R(t) \right] \right) \right]. \quad (\text{A.2})$$

Here, $N = 0, 1, 2, \dots$, $E_N = (N + 1/2)\hbar\omega_c$,

$$x_0 = x_0(t) = C \cos(\omega_c t) + D \sin(\omega_c t) - \omega_c \left[\sin(\omega_c t) \int^t d\tau f(\tau) \cos(\omega_c \tau) - \cos(\omega_c t) \int^t d\tau f(\tau) \sin(\omega_c \tau) \right] \quad (\text{A.3})$$

where C and D are integral constants,

$$\chi_N(x) = (2^N N! \pi^{1/2} l)^{-1/2} e^{-(x/l)^2/2} H_N(x/l) \quad (\text{A.4})$$

and

$$R(t) = \frac{1}{2} \int^t d\tau \left[\left(\frac{dx_0(\tau)}{d\tau} \right)^2 - \omega_c^2 [f(\tau) + x_0(\tau)]^2 \right]. \quad (\text{A.5})$$

Appendix B

The time-dependent component of the Schrödinger equation, equation (3), along the xy -plane is

$$i\hbar \frac{\partial \Phi(x, t)}{\partial t} = H_{xy}(t) \Phi(x, t) = \left[-\frac{\hbar^2}{2m^*} \left(\frac{\partial}{\partial x} - i \frac{eA_x(t)}{\hbar} \right)^2 + \frac{m^*}{2} \omega_c^2 (x + l^2 k_y)^2 \right] \Phi(x, t). \quad (\text{B.1})$$

Setting $x = x' + \alpha$ and $\alpha = \alpha(t) = -(e/m^*) \int^t d\tau A_x(\tau)$, equation (B.1) becomes

$$i\hbar \frac{\partial \Phi(x', t)}{\partial t} = \left[-\frac{\hbar^2}{2m^*} \frac{\partial^2}{\partial x'^2} + \frac{m^*}{2} \omega_c^2 [x' + l^2 k_y + \alpha]^2 + \frac{[eA_x(t)]^2}{2m^*} \right] \Phi(x', t). \quad (\text{B.2})$$

Assuming $\Phi(x', t) = \phi(x', t) \exp[-(i/\hbar) \int^t d\tau (eA_x(\tau))^2/2m^*]$, equation (B.2) reads

$$i\hbar \frac{\partial \phi(x', t)}{\partial t} = \left[-\frac{\hbar^2}{2m^*} \frac{\partial^2}{\partial x'^2} + \frac{m^*}{2} \omega_c^2 [x' + f(t)]^2 \right] \phi(x', t) \quad (\text{B.3})$$

where $f(t) = \alpha(t) + l^2 k_y$. The solution of equation (B.3) is presented in appendix A. Thus, the solution of equation (B.1) is given by

$$\Phi(x, t) = \chi_N(x - x_0 - \alpha) e^{-iE_N t/\hbar} e^{im^*[(x-x_0-\alpha)(dx_0/dt)+R_1(t)]/\hbar} \quad (\text{B.4})$$

where $x_0 = x_0(t)$ is given by equation (A.3) and

$$R_1(t) = \frac{1}{2} \int^t d\tau \left[\left(\frac{dx_0(\tau)}{d\tau} \right)^2 - \omega_c^2 [f(\tau) + x_0(\tau)]^2 - \left(\frac{eA_x(\tau)}{m^*} \right)^2 \right]. \quad (\text{B.5})$$

After: (i) introducing the initial condition $x - x_0(t) - \alpha(t) = x + l^2 k_y$, at $t = 0$ and (ii) using a condition that when the radiation field is absent (i.e., $F_0 = 0$): $x - x_0(t) - \alpha(t) = x + l^2 k_y$, we can determine the integral constants C and D in equation (A.3) and, thus, the solution of equation (3) can be obtained as equation (4).

Appendix C

For the LLs $N = 0, 1, 2, 3$, and 4, the factor $F_{Nm}(x)$ takes the forms

$$F_{0m}(x) = R_m(x) \quad (\text{C.1})$$

$$F_{1m}(x) = (1 - 2c)R_m(x) + c[R_{m+1}(x) + R_{m-1}(x)] \quad (\text{C.2})$$

$$F_{2m}(x) = (1 - 4c + 3c^2)R_m(x) + 2c(1 - c)[R_{m+1}(x) + R_{m-1}(x)] \\ + \frac{c^2}{2}[R_{m+2}(x) + R_{m-2}(x)] \quad (\text{C.3})$$

$$F_{3m}(x) = (1 - 6c + 9c^2 - 10c^3/3)R_m(x) + \frac{c}{2}(6 - 12c + 5c^2)[R_{m+1}(x) + R_{m-1}(x)] \\ + \frac{c^2}{2}(3 - 2c)[R_{m+2}(x) + R_{m-2}(x)] + \frac{c^3}{6}[R_{m+3}(x) + R_{m-3}(x)] \quad (\text{C.4})$$

and

$$F_{4m}(x) = (1 - 8c + 18c^2 - 40c^3/3 + 35c^4/12)R_m(x) \\ + c(4 - 12c + 10c^2 - 7c^3/3)[R_{m+1}(x) + R_{m-1}(x)] \\ + \frac{c^2}{2}(6 - 8c + 7c^2/3)[R_{m+2}(x) + R_{m-2}(x)] + \frac{c^3}{2}(2 - c)[R_{m+3}(x) + R_{m-3}(x)] \\ + \frac{c^4}{24}[R_{m+4}(x) + R_{m-4}(x)]. \quad (\text{C.5})$$

Here,

$$c = \frac{E_{em}}{\hbar\omega} \omega_c^* \left[\frac{1 + \omega_c^*}{1 - \omega_c^*} - x \right] \quad (\text{C.6})$$

where $\omega_c^* = \omega_c/\omega$, $x_{\pm} = \omega_c^* \pm (1 \pm \omega_c^*)x$, and

$$R_m(x) = \left(\frac{1 + \omega_c^*}{|1 - \omega_c^*|} \right)^m \left(\frac{x_-}{x_+} \right)^{m/2} e^{-c} I_m \left(\frac{|E_{em}|}{\hbar\omega} \sqrt{x_+ x_-} \right) \quad (\text{C.7})$$

with $I_m(x)$ being the modified Bessel function.

References

- [1] See, e.g., Prange R E and Girvin S M 1987 *The Quantum Hall Effect* (New York: Springer)
- [2] Feldhaus J and Weise H (ed) 2000 *Free Electron Lasers 1999* (Amsterdam: Elsevier)
- [3] Koenraad P M, Lewis R A, Waumans L R C, Langerak C J G M, Xu W and Wolter J H 1998 *Physica B* **256–8** 268
- [4] Koenraad P M *et al* unpublished experimental results
- [5] Xu W 1997 *J. Phys.: Condens. Matter* **9** L591
- [6] Pottier N and Calecki D 1982 *Physica A* **110** 471

- [7] See, e.g., Shankar R 1980 *Principles of Quantum Mechanics* (New York: Plenum)
- [8] See, e.g., Mattuck R D 1976 *A Guide to Feynman Diagrams in the Many-Body Problem* (New York: McGraw-Hill)
- [9] Jauho A P and Johnsen K 1996 *Phys. Rev. Lett.* **76** 4576
Johnsen K and Jauho A P 1998 *Phys. Rev. B* **57** 8860
- [10] Xu W and Vasilopoulos P 1995 *Phys. Rev. B* **51** 1694
Xu W, Vasilopoulos P, Das M P and Peeters F M 1995 *J. Phys.: Condens. Matter* **7** 4419
- [11] See, e.g., Seeger K 1991 *Semiconductor Physics—an Introduction* (Berlin: Springer)
- [12] Xu W 1998 *Phys. Rev. B* **57** 15 282
- [13] Xu W 1997 *Semicond. Sci. Technol.* **12** 1559
- [14] Nordstrom K B, Johnsen K, Allen S J, Jauho A P, Birnir B, Kono J, Noda T, Akiyama H and Sakaki H 1998 *Phys. Rev. Lett.* **81** 457
- [15] See, e.g., Ando T, Fowler A B and Stern F 1982 *Rev. Mod. Phys.* **54** 437
- [16] See, e.g., Eisenstein J 1987 *Interfaces, Quantum Wells, and Superlattices (NATO Advanced Study Institute, Series B: Physics, vol 179)* (New York: Plenum) p 271
- [17] See, e.g., Smith T P, Goldberg B B, Stiles P J and Heiblum M 1985 *Phys. Rev. B* **32** 2696
- [18] Gornik E, Lassning R, Strasser G, Störmer H L, Gossard A C and Wiegmann W 1985 *Phys. Rev. Lett.* **54** 1820
- [19] Husimi K 1953 *Prog. Theor. Phys.* **9** 381